^{1}H NMR Investigation of Manganese Peroxidase from *Phanerochaete chrysosporium*. A Comparison with Other Peroxidases

Lucia Banci,[‡] Ivano Bertini,*[,‡] Elizabeth A. Pease,[§] Ming Tien,[§] and Paola Turano[‡]

Department of Chemistry, University of Florence, Florence, Italy, and Department of Molecular and Cell Biology, The Pennsylvania State University, University Park, Pennsylvania 16802

Received February 28, 1992; Revised Manuscript Received June 15, 1992

ABSTRACT: ^{1}H NMR spectra at 200- and 600-MHz of manganese peroxidase from *Phanerochaete chrysosporium* and of its cyanide derivative are reported. The spectrum of the native protein is very similar to that of other peroxidases. The assignment of the spectrum of the cyanide derivative has been performed through 1D NOE, 2D NOESY, and COSY experiments. This protein is very similar to lignin peroxidase, the only meaningful difference being the shift of Hδ2 of the proximal histidine. The spectra of the cyanide derivative of these two proteins are compared with those of horseradish peroxidase and cytochrome *c* peroxidase. The shift pattern of the protons of the proximal histidine is discussed relative to the structural properties which affect the Fe^{3+}/Fe^{2+} redox potential.

Lignin peroxidase (LiP) and manganese peroxidase (MnP), discovered in the filamentous fungus *Phanerochaete chrysosporium*, catalyze the initial depolymerization of the lignin polymer (Tien & Kirk, 1983; Glenn et al., 1983). These enzymes have now been found in other lignin-degrading fungi and have been demonstrated to depolymerize lignin in vitro (Hammel & Moen, 1991; Wariishi et al., 1991). Both peroxidases contain a pentacoordinated, essentially high-spin ferric heme and utilize H_2O_2, also produced by the fungus, to oxidize a variety of organic and inorganic substrates (Tien, 1987; Kirk & Farrell, 1987). cDNA sequencing reveals that residues thought to be essential for peroxidase activity are conserved in both peroxidases (Pease et al., 1989; Pribnow et al., 1989; Tien & Tu, 1987). One residue is the proximal histidine which is the axial ligand of the heme. The other residue is also a histidine (distal) and is thought to be involved in the reaction of the enzyme with H_2O_2. The heme is formally oxidized to iron(IV) and to a cation radical upon reaction with H_2O_2. The two-electron-oxidized enzyme, referred to as compound I, returns to resting enzyme by oxidizing two substrate molecules (S), sequentially, going through an one-electron-oxidized intermediate, referred to as compound II:

$$\text{P[Fe(III)] (peroxidase)} + H_2O_2 \rightarrow \text{P[O=Fe(IV)–R}^{\bullet+}\text{]} \text{ (compound I)} + H_2O$$

$$\text{P[O=Fe(IV)–R}^{\bullet+}\text{]} + S \rightarrow \text{P[O=Fe(IV)]} \text{ (compound II)} + S^{\bullet}$$

$$\text{P[O=Fe(IV)]} + S \rightarrow \text{P[Fe(III)]} + S^{\bullet}$$

The radical $S^{\bullet}$ can undergo a variety of nonenzymatic reactions.

Peroxidases from numerous sources have been extensively characterized. Although they all share a common catalytic cycle as shown above, they differ in the nature of the substrates oxidized (S) and consequently in their function. Both LiP and MnP are unique in their substrate profile. Their substrates are characterized by high reduction potentials which cannot be oxidized by other peroxidases (Kersten et al., 1990). Lignin peroxidases are capable of catalyzing the oxidation of methoxybenzenes with redox potentials greater than 1.5 V, generating aryl cation radicals (Hammel et al., 1986). Mn peroxidases catalyze the oxidation of divalent manganese to trivalent manganese at a redox potential of 1.5 V (Glenn et al., 1986).

Despite a wealth of mechanistic information on peroxidases, relatively little structural information is available. This is because the X-ray structure is known for only one peroxidase, cytochrome *c* peroxidase (CcP) (Poulos & Kraut, 1980). Figure 1 shows the active-site structure of CcP. ^{1}H NMR spectroscopy has proved to be a valuable tool for characterizing the active-site structure of numerous peroxidases (Gonzales-Vergara et al., 1985; Goff, 1983; Satterlee, 1987; Morishima et al., 1977; Thanabal et al., 1986, 1988b and references therein; Banci et al., 1991b; de Ropp et al., 1991a). Protons near the heme iron experience large hyperfine shifts. However, the high-spin nature of these systems gives rise to signals with large line width (La Mar, 1979; Bertini & Luchinat, 1986). In contrast, the cyanide complexes contain low-spin iron(III) ($S = {}^1/_2$) with short electron relaxation time and provide sharp ^{1}H NMR signals and therefore have been extensively characterized by ^{1}H NMR spectroscopy (Satterlee et al., 1983, 1990, 1991; Satterlee & Erman, 1991; Banci et al., 1991a,b; Thanabal et al., 1987a,b, 1988a; Lukat et al., 1989; de Ropp et al., 1991a,b; Yamamoto et al., 1989, 1990). Of the peroxidases studied, the majority of the protons of the heme and those of the axial and the distal histidines have been assigned. The nonexchangeable signals of an arginine residue in the distal site have been assigned for HRP (Thanabal et al., 1987b) whereas only some signals of this residue have been tentatively assigned for the other proteins (Banci et al., 1991b; Satterlee & Erman, 1991; Satterlee et al., 1991). Some signals of a leucine residue in the proximal site have also been assigned. The shift values of the Hε1 signal of the proximal histidine in the cyanide derivative vary from one protein to another as well as the shift separation of the β-CH_2 signals. Such patterns have been tentatively related to the structural and redox properties of the proteins (Banci et al., 1991b).

We report here a ^{1}H NMR investigation of MnP (isoenzyme H4, with pI = 4.5), both in the high- and low-spin form. Our methodology includes 2D NOESY and COSY spectros-

* Author to whom correspondence should be addressed.
‡ University of Florence.
§ The Pennsylvania State University.

0006-2960/92/0431-10009$03.00/0

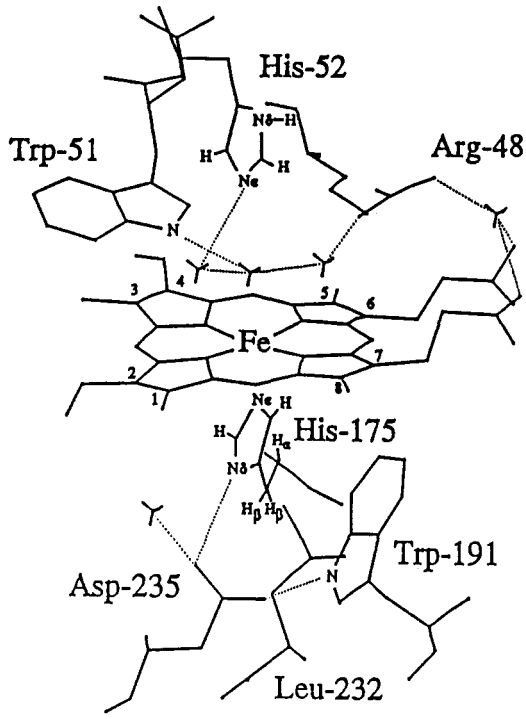

FIGURE 1: Structure of the heme pocket in CcP, as obtained from the X-ray structure (Poulos & Kraut, 1980). The side below the heme ring represents the proximal side, while that above is referred to as the distal side.

copy, as well as 1D NOE when high sensitivity and resolution is necessary. The application of 2D NMR techniques to these paramagnetic proteins of medium/large size (MW $\simeq$ 40 000) represents a frontier in the structural investigation of such systems and indeed some valuable information has already been obtained (de Ropp et al., 1991a,b; Banci et al., 1991a,b; Satterlee & Erman, 1991; Satterlee et al., 1991). The spectra of MnP are compared to those of other peroxidases. This approach has provided valuable information on structural differences between these peroxidases.

EXPERIMENTAL PROCEDURES

Preparation of Manganese Peroxidase. MnP was isolated by PSBL-1, an overproducing strain of *P. chrysosporium* (Tien & Myer, 1990). The MnP fractions, isoenzymes H3, H4, and H5, were obtained from the Mono Q column as previously described (Kirk et al., 1985) and further purified on a blue agarose column (Glenn & Gold, 1985). The H4 fraction (pI = 4.5) was further purified by preparative flatbed isoelectric focusing. Isoelectric focusing gels were run using a Pharmacia/LKB Multiphor II apparatus. Gels were made of Sephadex and ampholines to provide a pH range from 3.5 to 5.0. Enzyme preparations were greater than 99% pure as determined by SDS–PAGE, analytical isoelectric focusing, and N-terminal amino acid sequencing. MnP preparations typically exhibited R_Z values of 5 (A_{406}/A_{280}) and were quantitated using an extinction coefficient of 127 mM^{-1} cm^{-1} at 406 nm (Millis et al., 1989).

^1H NMR Spectroscopy. Spectra of MnP and MnP–CN^- [$\simeq$2 mM in 0.1 M phosphate buffer, pH 6.5] were recorded with Bruker MSL 200 and AMX 600 spectrometers. T_1 experiments have been performed at both 200 and 600 MHz, with the MODEFT (modified driven equilibrium Fourier transform) pulse sequence (Hochmann & Kellerhalls, 1980) and with the inversion–recovery pulse sequence (Vold et al., 1968). All other spectra at 200 MHz were taken by using a super WEFT (water-eliminated Fourier transform) pulse sequence (Inubushi & Becker, 1983) with a recycle delay of 85 and 220 ms for high- and low-spin species, respectively. The identification of the two nonexchangeable protons of the proximal histidine ring in the cyanide adduct was obtained by using a super WEFT pulse sequence with a recycle delay of 10 ms and a τ value of 5 ms. The nuclear Overhauser effect (NOE) difference spectra were collected as previously described (Banci et al., 1989).

NOESY and COSY spectra were recorded at 600 MHz using presaturation to eliminate the water signal. Phase-sensitive NOESY spectra (Macura et al., 1982) were recorded at mixing times of 15 ms to avoid spin diffusion, using the TPPI method (Marion & Wüthrich, 1983). A total of 512 experiments was collected with 1K data points in the F_2 direction. The data were multiplied in both dimensions by a sine-squared bell window function with phase shift of 45° and were zero-filled to obtain 1K × 1K real data points. Magnitude COSY (Aue et al., 1976) experiments provide one of the best sequences for detecting scalar connectivities between paramagnetically shifted signals (Yu et al., 1990; Bertini et al., 1991). In the present case, the best results were obtained by recording 512 experiments with 1K data points in the F_2 direction, processed in both dimensions by a pure sine-squared bell window function and zero-filled to obtain 1K × 1K real data points. Magnitude experiments exhibited a sizeable broadening of the resonances, which prevents the resolution of possible cross-peaks between close signals. In such cases, TPPI experiments were performed over larger number of data points in both dimensions. In the present study, TPPI COSY experiments permitted the resolution of cross-peaks between a signal and other two signals of 50-Hz line width, separated by 130 Hz. These experiments were performed by recording 2K experiments with 1K data points in the F_2 direction.

Steady-state NOEs provide the highest sensitivity for revealing magnetization transfer and also the largest resolution for detecting connectivities between closely spaced signals (Neuhaus & Williamson, 1989). In the present system the NOE, η_i, observed for a signal i upon saturation of a signal j, is given by

$$\eta_i = -\left(\frac{\hbar^2\gamma^4}{10r_{ij}^6}\tau_c\right)T_{1_{isel}}$$

where τ_c is the reorientational correlation time, r_{ij} is the distance between H_i and H_j, and $T_{1_{isel}}$ is the selective T_1 of signal i. If τ_c is determined by the protein tumbling, it is estimated to be 2.2×10^{-8} s through the Stock–Einstein equation (Bertini & Luchinat, 1986).

RESULTS

Resting State MnP. The 600-MHz ^1H NMR spectrum of the high-spin MnP at 298 K in H_2O is shown in Figure 2A. The broad signal a at 91.8 ppm disappears when the spectrum is recorded in D_2O (Figure 2B). The spectrum shows, resolved from the diamagnetic envelope (1) two signals, A and B, of intensity 3, (2) two overlapping signals, D and E, each of intensity 3, and (3) several signals, F–L, of intensity 1. Upfield signals are observed at –3.1, –5.9, –6.9, and –10.4 ppm. The spectrum closely resembles that of high spin LiP (Figure 2C,D).

The T_1 values at 200 MHz for these proteins are also reported in Figure 2. The downfield-shifted signals of intensity 3 are due to the CH_3 groups of the heme. The signals of intensity 1 are due to the Hα of the vinyl and propionate moieties of the heme and to the Hβ protons of the proximal histidine. This assignment is based on similarity of the shift value patterns with other peroxidases such as HRP (Thana-

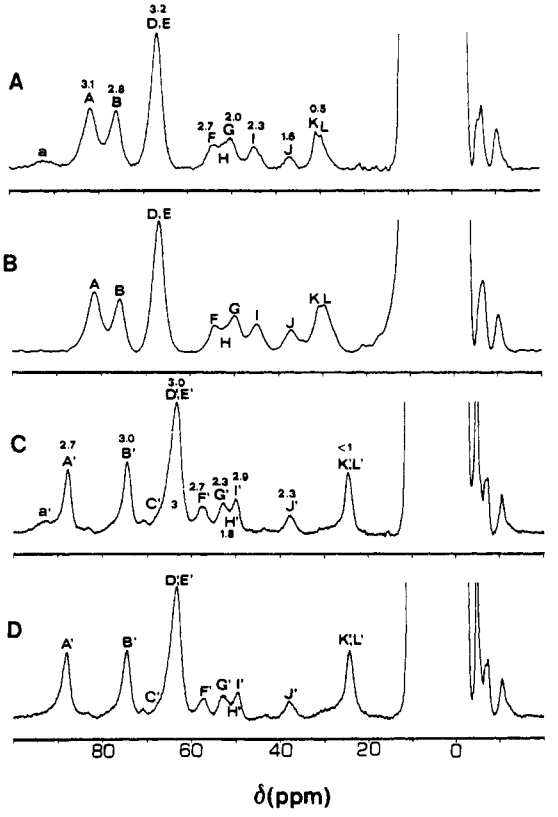

FIGURE 2: 600-MHz ^{1}H NMR spectra at 298 K of (A) MnP in H_2O, (B) MnP in D_2O, (C) LiP in H_2O, and (D) LiP in D_2O. All the samples are in 0.1 M phosphate buffer, pH 6.5. The numbers above the signals indicate their T_1 values (measured at 200 MHz) in milliseconds.

bal et al., 1986, 1988b), CcP (Satterlee et al., 1983), and LiP (Banci et al., 1991b; de Ropp et al., 1991a). Due to the similarity of the spectrum of MnP with that of LiP, to the intrinsic difficulties of characterizing a system with broader lines than other peroxidases, and to the relatively low concentration of the sample, we did not pursue a further detailed characterization of this system.

An interesting feature of the ^{1}H NMR spectrum of the high-spin form of MnP is the presence of a broad signal, far downfield shifted, which is exchangeable. A similar signal had been observed in other high-spin iron(III) heme proteins and assigned to Hδ1 of the proximal histidine (Lukat et al., 1989; La Mar & de Ropp, 1979). Its exchange behavior varies with these different hemeproteins. In the case of metmyoglobin, the signal disappears as the sample is exchanged in D_2O (La Mar & de Ropp, 1979) whereas, for HRP, the signal maintains its intensity even after incubation in D_2O for several weeks (La Mar & de Ropp, 1979). In the case of MnP, this signal disappears when the sample is placed in D_2O. However, the present signal is detectable only in the spectrum recorded at 600 MHz but not at 200 MHz. This indicates that the exchange rate with the bulk water should be slower than 5×10^4 s^{-1} but faster than 2×10^4 s^{-1}. A similar behavior is observed also in the case of LiP, for which this signal was not observed in the spectrum recorded at 200 MHz (Banci et al., 1991b), but it is detected in the spectrum recorded at 600 MHz (Figure 2C,D). This observation sets the exchange rate with the bulk water in the same range values as for MnP. The exchange rate of this proton then results to be in the order LiP $\simeq$ MnP > metmyoglobin > HRP. It could be determined by the accessibily of the solvent to the proximal histidine NH.

Cyanide Adduct of MnP. The ^{1}H NMR spectrum at 200 MHz of the cyanide adduct of MnP is shown in Figure 3. Also shown in Figure 3 are the spectra of the CN^- adduct of other peroxidases. The shift and T_1 values for the CN^- adducts of these peroxidases are reported in Table I.

Figures 4 and 5 show the COSY and NOESY (mixing time, 15 ms) spectra obtained at 600 MHz and 307 K. The COSY map of MnP–CN^-, collected in D_2O, clearly shows some well-resolved scalar connectivities outside of the diamagnetic envelope. The pattern identified by cross-peaks 15, 16, and 22 allowed us to assign signal E as Hα and signals V and W as $H\beta_{trans}$ and $H\beta_{cis}$ of a vinyl heme group. Indeed, the J values are in the order of Hα–$H\beta_{trans}$ > Hα–$H\beta_{cis}$ > $H\beta_{trans}$–$H\beta_{cis}$. The relative T_2^{-1} values are in the order Hα > Hβ. The intensity of the cross-peaks is larger with the larger J values and the smaller T_2^{-1} values. Therefore, the intensity of cross-peaks in the order 16 > 15 > 22 is consistent with the above assignment, which is similar to that proposed for other peroxidases (Thanabal et al., 1987a; Satterlee & Erman, 1991; Satterlee et al., 1991; Banci et al., 1991a,b; de Ropp et al., 1991a). The NOESY pattern is also interpreted on this basis with a strong connectivity between geminal protons (22), a relatively intense cross-peak between Hα and $H\beta_{cis}$ (15), and a weak cross-peak between Hα and $H\beta_{trans}$ (16). The second heme vinyl group is not clearly apparent in this spectrum. Possible candidates for the Hβ protons are signals X and Y, which show a composite cross-peak with the possible Hα, signal J at 8.6 ppm. Their shift values are similar to those of the corresponding signals in other peroxidases (Satterlee et al., 1987, 1990, 1991; Satterlee & Erman, 1991; Thanabal et al., 1987a; Lukat et al., 1989; Banci et al., 1991a,b; de Ropp et al., 1991a). Unfortunately, the poor resolution of the present magnitude COSY experiment prevents us from resolving signals X and Y. We, therefore, performed a TPPI COSY experiment with a larger number of data points. This permitted resolution of scalar coupling between X and J and between Y and J. The connectivity between X and Y is not, however, resolved in any 2D experiment (COSY and NOESY).

We then performed a 1D NOE experiment. Due to the close position of these two signals (130 Hz apart), particular care should be paid when setting up the experiment in order to prevent off-resonance effects which could mask the real NOE effect. The experiment was performed by saturating signal X and by placing the decoupler frequency in the reference spectrum upfield with respect to Y, at a symmetric position with respect to X. In this way all the off-resonance effects on signal Y in the saturated spectrum are exactly balanced by those in the reference spectrum, thus allowing the detection of even a small NOE. In this experiment, by saturating signal X, a NOE of about 40% is observed on Y. In the two-spin approximation and assuming $\tau_c = 2.2 \times 10^{-8}$ s, a proton–proton distance of 2.1 Å can be calculated. This value is higher than expected for two geminal protons. However, this NOE extent could give the correct distance value (1.88 Å) if the correlation time τ_c for this group is half the protein rotational correlation time, as a result of the mobility of the vinyl moiety. This effect has already been observed in the case of metmyoglobin–CN^- for a vinyl group (Ramaprasad et al., 1984) and in the case of metmyoglobin–N_3^- for a propionate group (Yamamoto et al., 1991). All these measurements indicate that X and Y are geminal protons and that they belong to the same moiety with signal J. We therefore assign signal J as Hα, signal X as $H\beta_{cis}$, and signal Y as $H\beta_{trans}$ of a vinyl moiety. These assignments are consistent with the intensity of the cross-peaks in both the NOESY and COSY experiments.

The CH_3 signal A gives, among the many dipolar connectivities, cross-peaks with signals E (6), V(4), and W (3). These latter signals are those which have already been assigned to

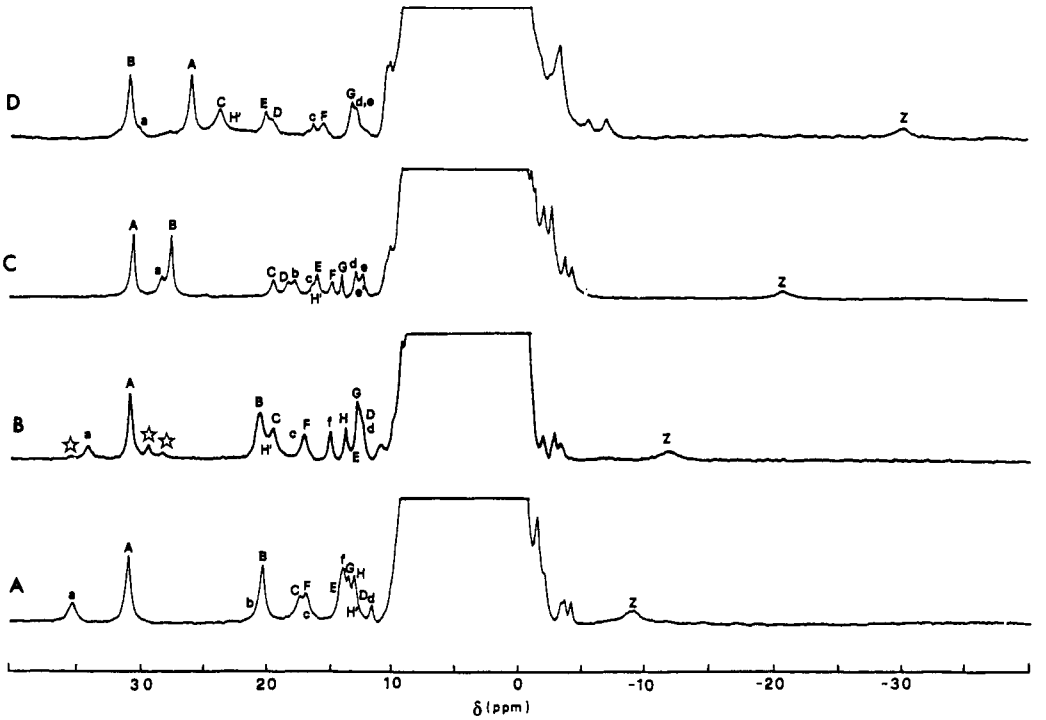

FIGURE 3: 200-MHz and 301 K ^{1}H NMR spectra of the CN^- adducts of (A) LiP, acetate buffer, pH 5; (B) MnP, phosphate buffer, pH 6.5; (C) CcP, phosphate buffer, pH 6.3; (D) HRP, phosphate buffer, pH 6.3. Signals indicated by stars in spectrum B are due to impurities, as indicated by their fractional intensity and by the different relative intensity in different samples of MnP analyzed in the present study.

Table I: Chemical Shift and Nonselective T_1 Values at 200 MHz Observed for Paramagnetically Shifted Resonances for the Cyanide Derivatives of MnP (298 K), LiP (301 K), CcP (301 K), and HRP (301 K)[a] and the Intercept Values at Infinite Temperature

	MnP–CN^-			LiP–CN^-			CcP–CN^-		HRP–CN^-			
assignment	shift (ppm)	T_1[b] (ms)	int (ppm)	shift (ppm)	T_1 (ms)	int[c] (ppm)	shift (ppm)	T_1 (ms)	shift (ppm)	T_1 (ms)	int[d] (ppm)	signal
2-Hα	8.6[e]	*f*	13.1	8.5[e]	*f*		7.1[g]	*f*	5.3[h]	*f*	9.2	J
2-Hβ_{cis}	−3.4[e]	*f*	6.4	−3.6[e]	150	6.2	−3.7[g]	*f*	−1.6[h]	*f*	5.8	X
2-Hβ_{trans}	−3.2[e]	*f*	7.8	−4.1[e]	130	8.0	−3.0[g]	*f*	−2.7[h]	*f*	6.6	Y
α-meso	−1.1[e]	*f*	20.3	1.1[e]	*f*	13.5			1.9[i]	*f*		α
3-CH_3	30.7	67	−18.2	31.0	44	−5.9	30.6	40	26.0	57	−1.0	A
4-Hα	12.7	*f*	2.1	14.2	*f*	5.9	16.0	60	20.1	96	7.6	E
4-Hβ_{cis}	−2.8[e]	165	7.6	−3.2[e]	140	4.5	−3.8[g]	*f*	−3.3[h]	*f*	5.5	W
4-Hβ_{trans}	−1.8[e]	140	7.2	−2.0[e]	*f*	4.4	−2.1[g]	*f*	−2.2[h]	*f*	4.4	V
7-Hα	12.5	70	−1.4	13.0	*f*	2.0	18.3	45	19.6	83	5.7	D
7-Hα'	8.0[e]	*f*	7.9	9.2[e]	*f*	4.9	6.4[g]	*f*	9.7[h]	*f*	9.0	I
8-CH_3	20.4	92	−1.2	20.4	65	3.2	27.6	39	31.0	44	−0.8	B
δ-meso	7.0[e]	*f*	11.8	7.6[e]	*f*	11.1			6.3[i]	*f*	12.4	δ
NH_p prox. His	12.4	*f*	−1.7	11.6	81	3.9	12.9	110	12.9	238	1.0	d
Hβ prox. His	19.5	53	−10.0	17.4	41	−4.0	19.4	34	23.7	21	−9.8	C
Hβ' prox. His	16.9	86	−7.8	17.0	*f*	−3.4	14.8	34	15.6	41	−4.7	F
Hδ1 prox. His	15.1	29		14.0	*f*		10.2[j]	*f*	9.9[j]	*f*		f
Hϵ1 prox. His	−11.8	2.5	5.6	−9.0	3.0	−5.1	−20.6	2.5	−29.9	2.7	11.0	Z
Hδ2 prox. His	20.3	≤3		13.3	≤3		15.8	≤3	23.1	≤3		H′
Hϵ2 dist. His[k]	34.2	≃15		35.2	11		28.4	7	31.0	*d*		a

[a] Lowercase letters indicate exchangeable protons. [b] For T_1 values, the error is ±20%. [c] Taken from de Ropp et al. (1991a). [d] Taken from Thanabal et al. (1987a,b, 1988). [e] The shift value was measured from the 2D maps obtained at 600 MHz and the same temperature (Banci et al., 1991b). [f] Not measured because the signal is in a complex envelope. [g] The shift value was measured from the 2D maps obtained on MKT–IGCcP–CN^- at 600 MHz and 298 K (Banci et al., 1991a). [h] Shift value at 308 K (Thanabal et al., 1987a). [i] Shift value at 328 K (Thanabal et al., 1987a). [j] The shift value was measured in NOE difference spectra (Banci et al., 1991a; Thanabal et al., 1988a). [k] For the assignment of the other signals from the distal side protons, see the text.

a vinyl group. Therefore signal A is either 3-CH_3 or 1-CH_3. The CH_3 signal B gives a dipolar connectivity with signal D (8), which is intensely dipolar coupled with signal I (18). Both of the resolved CH_3 signals do not give any connectivity with the vinyl moiety identified by signals J, X, and Y. The contact shift contribution on the protons of the heme ring in the low-spin iron(III) systems is dominated by π delocalization, which influences pairwise shift values on substituents 180° apart (Shulman et al., 1971; La Mar & Walker, 1979; Thanabal et al., 1987a). Due to the similarity of the spectrum of this protein with those of other investigated peroxidases (Satterlee et al., 1987, 1990, 1991; Satterlee & Erman, 1991; Banci et al., 1991a,b; Thanabal et al., 1987a,b, 1988a; Lukat et al., 1989; de Ropp et al., 1991a), the same delocalization is presumably operative here. This means that signal B is due either to 8-CH_3 or to 5-CH_3. This then indicates that signals D and I are the Hα of a proprionate chain. Indeed a cross-peak is present in the COSY map of LiP–CN^- between the corresponding signals D and I (unpublished results from this lab).

Signal A shows other strong dipolar connectivities, detected in the NOESY map. In particular, it is coupled with signal

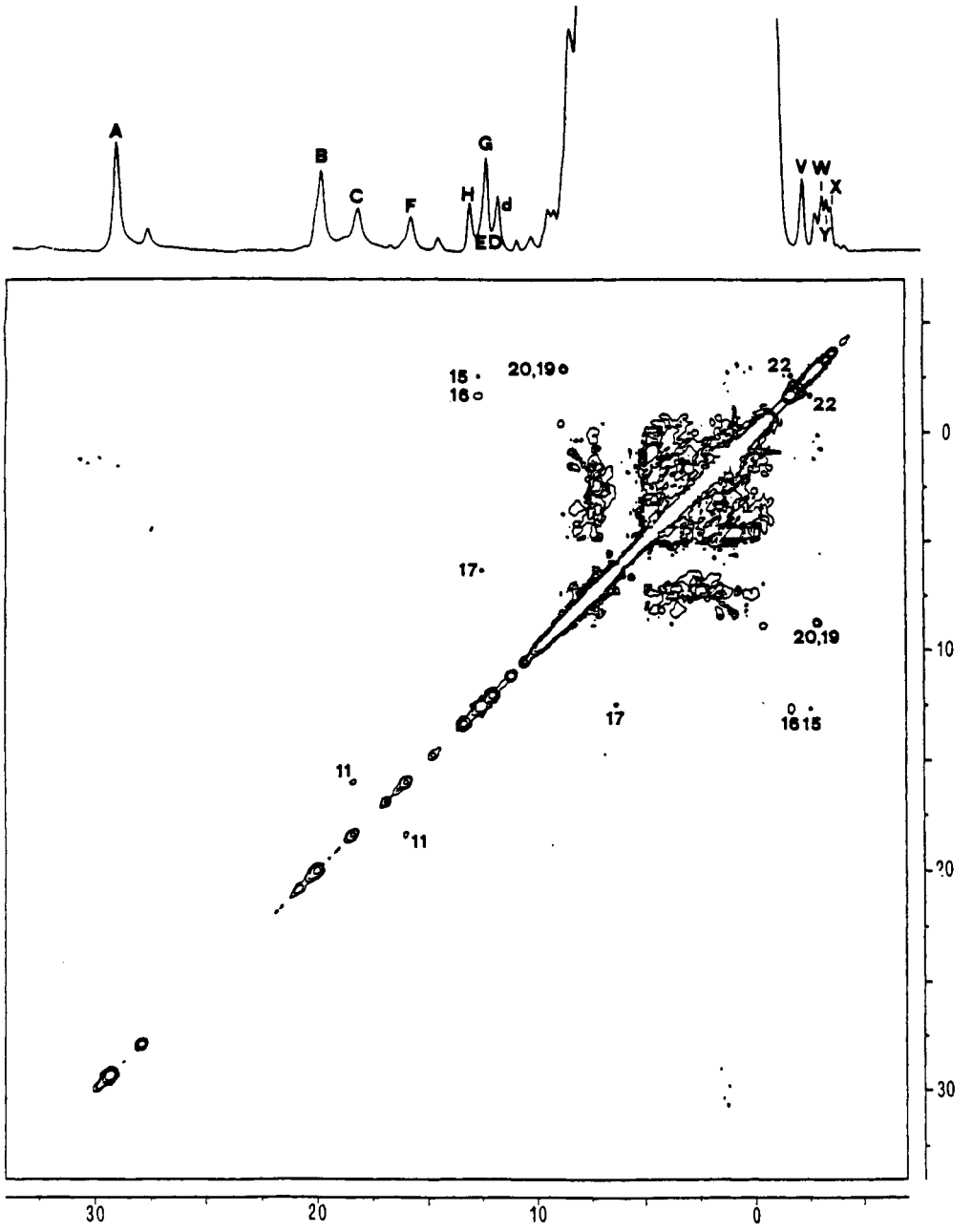

FIGURE 4: 600-MHz 307 K magnitute COSY spectrum in D_2O of MnP–CN^-. Cross-peak assignments: (11) Hβ proximal His; Hβ' proximal His; (15) 4-Hα, 4-Hβ_{cis}; (16) 4-Hα, 4-Hβ_{trans}; (17) G, K; (19, 20) 2-Hα, 2-Hβ_{cis}/2-Hα, 2-Hβ_{trans}; (22) 4-Hβ_{trans}, 4-Hβ_{cis}.

α, at −1.09 ppm at 298 K (cross-peak 5). The latter signal shows a strong temperature dependence in the NOESY experiments. Four different temperatures were examined; the intercept at infinite temperature is at 20.3 ppm. Signal α, in turn, is dipolarly coupled with signal J (21), assigned as Hα of a vinyl moiety. The temperature dependence, the shift value, and these connectivities allow us to assign signal α as the α-meso proton. This assignment then establishes that signal A is 3-CH_3, J, X, and Y are protons of 2-vinyl group, and signal B is due to 8-CH_3. The lack of connectivities between signal A and any proton of the 2-vinyl group could be explained by a different orientation of 2-vinyl with respect to that observed in LiP and HRP (Chart IA) but similar to that in CcP (Chart IB). It is possible, however, that a fast interconversion of the heme vinyl group between the two conformations shown in Chart IA,B reduces the size of the dipolar coupling, thus making undetectable an NOE already small in rigid systems. It is interesting to note that the order of the two downfield-shifted CH_3 signals in the low-spin form of MnP is the same as for CcP and LiP but is opposite to what is observed for HRP. As shown in Table I, the α-meso signal has a significantly higher intercept whereas the 3-CH_3 signal has a much more negative intercept at infinite temperature relative to other peroxidases. For all the other signals, the intercept values are in the usual range. Interestingly, the signals, whose shifts deviate from the linear $1/T$ dependence, originate from protons that are on the same side of the heme ring, close to the 2-vinyl group. The strong temperature dependence of the above signals could be a result of local effects, such as the mobility of the 2-vinyl group, as already discussed.

Signal B is dipolarly coupled with signal δ at 6.95 ppm (cross-peak 7), which shows a strong temperature dependence, with an intercept of 11.8 ppm. This could be due to another meso proton of the heme ring, the δ-meso.

Signal B, due to 8-CH_3, shows an interesting behavior when the protein is dissolved in D_2O. In the latter solvent, the signal is resolved into two components, with a relative intensity consistent with the presence of some residual water. This has already been observed in HRP–CN^- and had been attributed

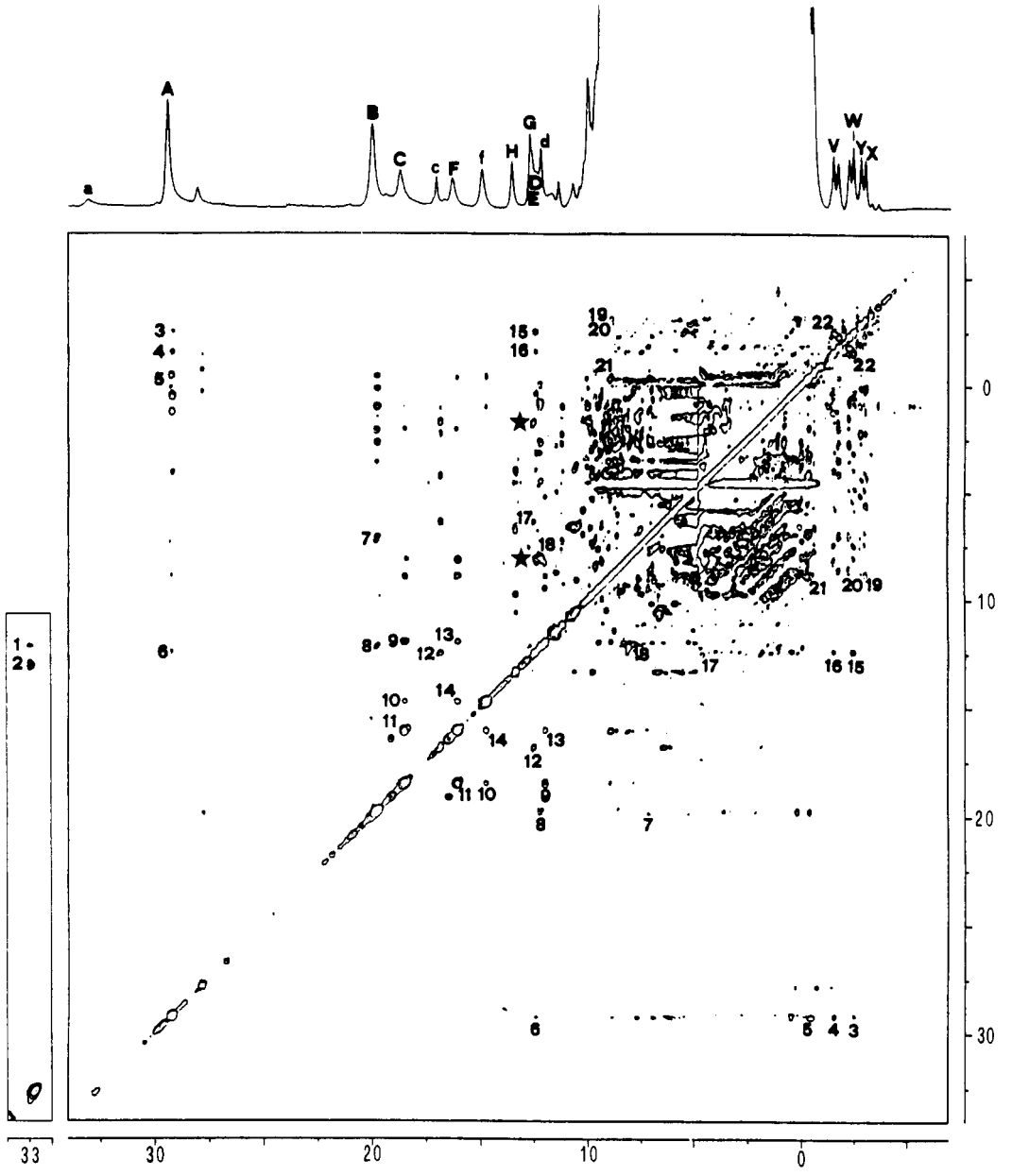

FIGURE 5: 600-MHz 307 K TPPI NOESY spectrum in H_2O of MnP–CN^- obtained with a 15-ms mixing time. Cross-peak assignments: (1) Hϵ2 distal His, G; (2) Hϵ2 distal His, H; (3) 3-CH_3, 4-Hβ_{cis}; (4) 3-CH_3, 4-Hβ_{trans}; (5) 3-CH_3, α-meso; (6) 3-CH_3; 4-Hα; (7) 8-CH_3; δ-meso; (8) 8-CH_3, 7-Hα; (9) Hβ proximal His, NH_p proximal His; (10) Hβ proximal His; Hδ1 proximal His; (11) Hβ proximal His; Hβ' proximal His; (12) c, G; (13) Hβ' proximal His, NH_p proximal His; (14) Hβ' proximal His; Hδ1 proximal His; (15) 4-Hα, 4-Hβ_{cis}; (16) 4-Hα, 4-Hβ_{cis}; (17) G, K; (18) 7-Hα, 7-Hα'; (19) 2-Hα, 2-Hβ_{cis}; (20) 2-Hα, 2-Hβ_{trans}; (21) 2-Hα, α-meso; (22) 4-Hβ_{trans}, 4-Hβ_{cis}. On the left is reported a different processing of the same experiment which allows the detection of cross-peaks 1 and 2.

to partial proton/deuteron interchange on a group interacting with the 8-CH_3 (Thanabal et al., 1988a).

In the COSY experiment reported in Figure 4, cross-peak 11 beween signals C and F identifies the β-CH_2 protons of the proximal histidine. They are also dipolarly coupled with signal d at 12.4 ppm (9, 13), which could be either the peptide NH or the Hα of the same residue. We prefer the first choice due to the similarity in shift with other peroxidases. Both signals C and F are further coupled (cross-peaks 10 and 14) with an exchangeable proton at 15.1 ppm (signal f), which we assign as Hδ1 of the proximal histidine. We assign the upfield signal Z as Hϵ1 of the proximal histidine on the basis of its shift and T_1 values as well as on NOE patterns. Saturation of signal Z provides 1D NOE on signal f, consistent with the above assignment. The other expected broad signal of proximal His (Hδ2; signal H' at 20.3) falls under other sharper signals and can be "extracted" by pulsing with extremely fast repetition rates. Figure 6 shows the Hϵ1 and Hδ2 signals of the proximal His in a series of cyanide adducts of peroxidases.

The exchangeable signal a gives NOESY cross-peaks with the nonexchangeable signals G (1) and H (2). The former gives dipolar connectivities, besides a, with exchangeable signal c (12). By analogy with HRP–CN^- and CcP–CN^-, the nonexchangeable signal (G), which is dipolarly coupled with two exchangeable protons, would be assigned as Hϵ1 of the distal His. The two exchangeable proton signals a and c are assigned as the two NH protons (Hϵ2 and Hδ1, respectively) of the same histidine. Again, by analogy with the above proteins, we would be inclined to assign signal H as Hδ2 of the distal histidine. Through ^{1}H NOE measurements and their buildup as a function of the saturation time of a, distances of 2.5 ± 0.1 Å have been calculated for the distance between protons a and H and between protons a and G. However, signal G gives rise to a COSY cross-peak (17) with a signal at 6.5 ppm, labeled K. This same connectivity was also observed in LiP–CN^- (Banci et al., 1991b). In order to rule out the possible origin from impurities, we have paid particular attention to this connectivity. Beside MCOSY experiments,

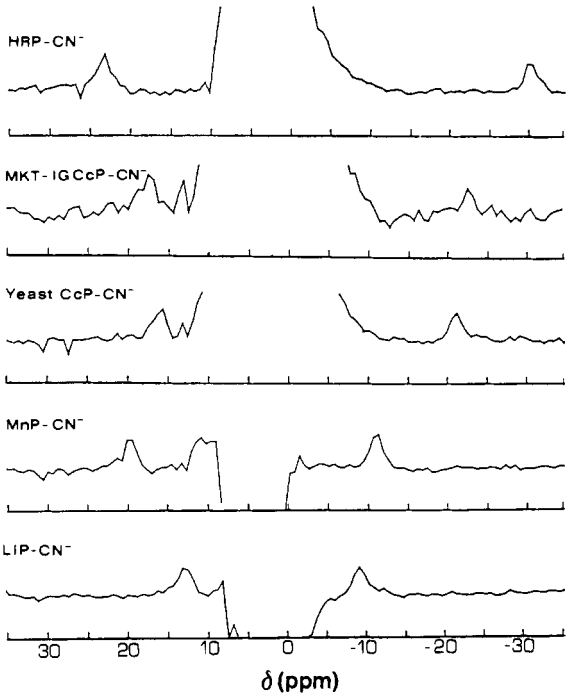

FIGURE 6: 200-MHz 301 K ^{1}H NMR spectra of different peroxidases obtained with a super WEFT pulse sequence with a recycle delay of 10 ms and a τ value of 5 ms. The downfield signal is due to Hδ2, and the upfield signal is due to Hϵ1 of the proximal histidine.

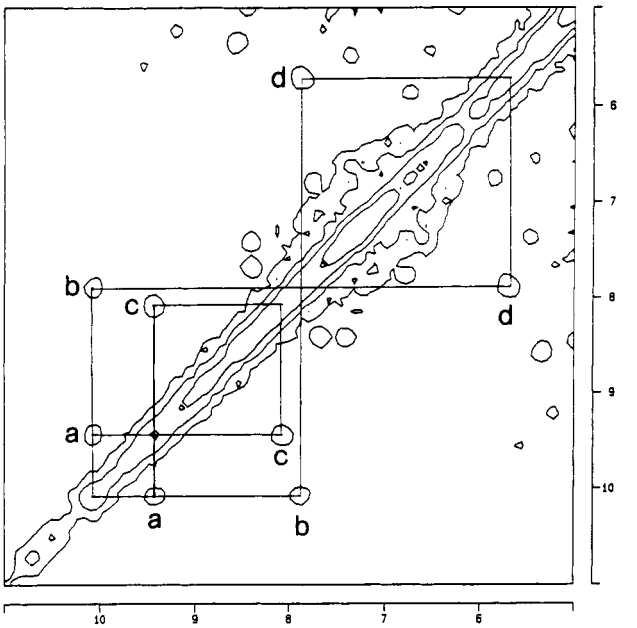

FIGURE 7: Aromatic region of the 600-MHz 300 K magnitude COSY spectrum of LiP–CN$^-$. Scalar connectivities between signals assigned to Phe 193 are connected by solid lines. Cross-peak assignment: (a) 4-H, 3-H; (b) 4-H, 5-H; (c) 3-H, 2-H; (d) 5-H, 6-H. Signals assigned to 2-H, 3-H, and 4-H show NOESY cross-peaks with the two β-CH$_2$ and with the ring NH signals of the proximal histidine in NOESY experiments obtained with a 15-ms mixing time (data not shown).

which were performed on two different preparations, we have also studied this connectivity with TPPI COSY experiments. Under these circumstances, G and K should be scalarly connected and should be assigned to a residue different from histidine. The presence of the cross-peak between G and K in LiP–CN$^-$ and MnP–CN$^-$ and its absence in CcP–CN$^-$ (which we have carefully checked) and HRP–CN$^-$ (as it appears from the data in the literature) indicates that the assignment may be different between the two sets of proteins. Finally, it should be noted that, while G does not show any other dipolar connectivity than with a and c in HRP–CN$^-$ and CcP–CN$^-$, it shows NOESY connectivities with K (17) and with at least two other signals (cross-peaks labeled with stars in Figure 5) in MnP–CN$^-$ and in LiP–CN$^-$ (Banci et al., 1991b; unpublished results from this lab).

In the proximal site, we have extended the comparison between MnP and LiP to groups other than the proximal His. An interesting feature in the COSY spectra of LiP–CN$^-$ is the presence of a well-resolved five-proton connectivity pattern in the region 6–10 ppm (see Figure 7). The same pattern is observed at two temperatures (300 and 310 K). It could be consistent with the assignment of these signals to a Phe residue, locked in a fixed position, so that the five ring protons are inequivalent. The sizeable spreading of their shift with respect to the typical diamagnetic values indicates that this residue experiences some isotropic shift contribution and therefore is in the proximity of the iron ion. The presence of NOESY cross-peaks between signals of the proximal His (the two β-CH$_2$ and the ring NH protons) and three protons of Phe (see the legend to Figure 7) and a comparison of the sequences of CcP (Takio et al., 1980; Poulos & Kraut, 1980) and LiP (Tien & Tu, 1987) suggest that this phenylalanine is Phe 193. From the cDNA sequence of MnP (Pease et al., 1989), it appears that a Phe residue is still present in the corresponding sequence

Chart I

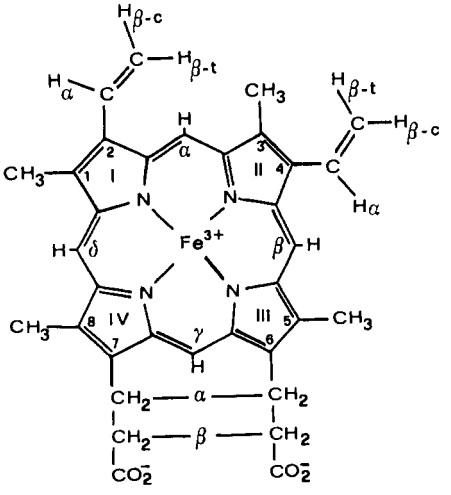

A

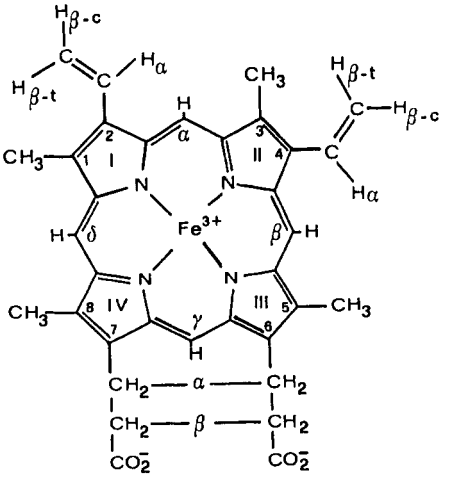

B

position. However, we do not detect an analogous COSY pattern from the same region of the COSY map in MnP–CN^-, which results to be more crowded. In addition, there are less dipolar connectivities between the proximal histidine protons and the aromatic region, suggesting a different reciprocal arrangement of proximal His and this Phe residue in MnP with respect to LiP.

DISCUSSION

The present results provide some structural information on MnP and has allowed comparison to analogous proteins. The NH of the proximal histidine, analogously to LiP, is solvent accessible and exchanges faster than in HRP. Indeed, in the former two proteins, the signal is observed in the high-spin species only at 600 MHz and not at 200 MHz, whereas in the latter it is always observed. For the rest of the spectrum, the similarity with LiP, with HRP (Morishima et al., 1977; Thanabal et al., 1988b; Gonzalez-Vergara et al., 1985), and CcP (Satterlee et al., 1983) is high and evident. The high-spin nature of the proteins prevents observation of the fine differences which are observed in their cyanide derivatives. In the latter case, the NMR spectra are indicative of a different arrangement of 2-vinyl compared to LiP and HRP. This could result from orientation of 2-vinyl similar to that of CcP (Chart IB) or could be due to a higher mobility of this group. Some differences are also present in the distal site although their firm interpretation is hard at the present stage.

The analysis of the shifts of the cyanide derivative may provide further information. The signals of protons of the heme residues which undergo the largest variation are at position 7, 8, and 4 (in the direction perpendicular to the orientation of the proximal histidine plane, which determines the in-plane magnetic axis). Parallel to these shift variations, we detect changes in the shifts of protons belonging to the proximal histidine. Particularly, the Hε1 signal varies dramatically from −30 ppm for HRP to about −10 ppm for LiP and MnP. We had empirically correlated this variation with the redox potential of the Fe(III)/Fe(II) couple in peroxidases (Banci et al., 1991b). The shift value of Hδ1 signal slightly increases from 9 to 15 ppm, and the Hδ2 signal decreases from 23 to 13 ppm in the series HRP, CcP, LiP and then increases again to 20 ppm in MnP. The shift value of Hδ1 is dominated by contact contributions, the dipolar shift being much smaller due to the large distance from the iron(III) ion. The shifts of Hδ2 and Hε1 are also experiencing a large dipolar contribution. The shifts of Hδ1, Hδ2, and Hε1 in metmyoglobin–CN^- are 20, −5, and 19 ppm, respectively. In this case, the proximal histidine has a much weaker hydrogen bond with a backbone carbonyl (Leu 89), and the couple Fe^{3+}/Fe^{2+} has the highest positive redox potential. The main discrepancies between LiP and MnP and the only relevant indications of some structural differences between the two proteins are provided by the shift of Hδ2 of the proximal histidine and by a different reciprocal arrangement of the proximal Phe residue with respect to the proximal His.

La Mar investigated the effect of the orientation of the magnetic susceptibility tensor axes in the molecular frame of metmyoglobin–CN^- with respect to the dipolar shifts of several resonances, including those of the proximal histidine (Emerson & La Mar, 1990). The dipolar shift values of Hε1 and Hδ2 of the proximal histidine have been found to be extremely sensitive to the orientation of the z axis, which, in the case of metmyoglobin–CN^-, has been proposed to be determined by the Fe–CN^- direction. A tilt of 15–20° in the z direction induces shift variations of 20–30 ppm in opposite directions for the two protons: a decrease in the upfield shift for Hε1 and a decrease in the downfield shift for Hδ2.

The observed pattern could therefore be ascribed to a tilt of the z axis in the CN^- derivative of the investigated peroxidases and of metmyoglobin. Such a tilt would be due to a different position of the distal histidine to which HCN is hydrogen bonded. It may also be that the orientation of the proximal histidine contributes to the fixing of the z axis. The latter case could be ascribed to steric requirements of the proximal cavity to the NH·O bond. This explanation would be more directly related to the redox properties of the systems and would account for changes in the contact contribution.

The strength of the hydrogen bond has a major influence on the basicity of the proximal histidine, which in turn strongly influences the reactivity and electron density of the heme. Histidines bound to iron porphyrins with increased hydrogen-bond strength stabilize the higher oxidation states of the heme iron (Doeff et al., 1983; Quinn et al., 1984; Smulevich et al., 1988, 1991), a property desired in peroxidases but not in the globins. However, a small amount of hydrogen bonding is necessary for globin function for it increases O_2 affinity, presumably by decreasing the dissociation rate of O_2 (Traylor et al., 1981b; Suslick et al., 1984) through polarization of the covalent Fe(II)–O_2 bond. This causes the transfer of electron density from the iron to the oxygen, imparting the oxycomplex with greater Fe^{3+}·O_2^- character (Traylor & Popovitz-Biro, 1988). However, increased hydrogen-bond strength can eventually promote the oxidation of the heme iron by O_2 to form higher valence intermediates (Mincey & Traylor, 1979). This latter property would stabilize the Fe^{4+} state found in peroxidases. The stronger hydrogen bonding also explains why peroxidases in general form very unstable oxycomplexes (Fe^{2+} state).

In myoglobin the Hδ1 proton of the proximal His forms a weak bond with the carbonyl of Leu 89 (Takano, 1977). In CcP, it forms a stronger hydrogen bond, with the negatively charged group Asp 235 (Poulos & Kraut, 1980; Smulevich et al., 1988). ^1H NMR studies on the reduced form suggested that the hydrogen bonding of Hδ1 proton could be even stronger in HRP (La Mar & de Ropp, 1982). If the ^1H NMR shift pattern of the proximal histidine protons in the CN^- derivative is taken as indicative of the hydrogen-bond strength, then LiP and MnP should have somewhat similar properties, with a weaker hydrogen bond compared to HRP and CcP. This is in agreement with electrochemical results (Millis et al., 1989). In accord with the hydrogen-bonding strength, the redox potentials of MnP and LiP are −93 and −142 mV (Millis et al., 1989). The redox potentials for metmyoglobin, CcP, and HRP are +46, −194, and −278 mV at pH 7, respectively. This pattern qualitatively correlates with the pattern of the shift values for the proximal histidine. The subtle differences between MnP and LiP, however, do not completely fit in the above scheme; the shift of Hδ2 of the proximal histidine indicates a further different conformation of this residue outside the pattern up to now discussed. The shift data will become more significant as more X-ray data become available.

ACKNOWLEDGMENT

We thank Prof. T. L. Poulos for discussing structural details on CcP and preliminary data on LiP. We acknowledge Dr. G. Smulevich for discussing the hydrogen bonding involving the proximal histidine.

REFERENCES

Aue, W. P., Bartholdi, E., & Ernst, R. R. (1976) *J. Chem. Phys. 64*, 2229–2246.

Banci, L., Bertini, I., Luchinat, C., Scozzafava, A., Piccioli, M., & Turano, P. (1989) *Inorg. Chem. 28*, 4650–4656.

Banci, L., Bertini, I., Turano, P., Ferrer, J. C., & Mauk, A. G. (1991a) *Inorg. Chem. 30*, 4510–4516.
Banci, L., Bertini, I., Turano, P., Tien, M., & Kirk, T. K. (1991b) *Proc. Natl. Acad. Sci. U.S.A. 88*, 6956–6960.
Bertini, I., & Luchinat, C. (1986) *NMR of Paramagnetic Molecules in Biological Systems*, Benjamin/Cummings, Menlo Park, CA.
Bertini, I., Capozzi, F., Luchinat, C., & Turano, P. (1991) *J. Magn. Reson. 95*, 244–252.
de Ropp, J. S., La Mar, G. N., Wariishi, H., & Gold, M. H. (1991a) *J. Biol. Chem. 266*, 15001–15008.
de Ropp, J. S., Yu, L. P., & La Mar, G. N. (1991b) *J. Biomol. NMR 1 1*, 175–190.
Doeff, M. M., Sweigart, D. A., & O'Brien, P. (1983) *Inorg. Chem. 22*, 851–852.
Emerson, D. S., & La Mar, G. N. (1990) *Biochemistry 29*, 1556–1566.
Glenn, J. K., & Gold, M. H. (1985) *Arch. Biochem. Biophys. 242*, 329–341.
Glenn, J. K., Morgan, M. A., Mayfield, M. B., Kuwahara, M., & Gold, M. H. (1983) *Biochem. Biophys. Res. Commun. 114*, 1077–1083.
Glenn, J. K., Akileswaran, L., & Gold, M. H. (1986) *Arch. Biochem. Biophys. 251*, 688–696.
Goff, H. M. (1983) in *Iron Porphyrins* (Lever, A. B. P., & Gray, H. B., Eds.) Vol. 1, pp 237–281, Addison-Wesley, Reading, MA.
Gonzalez-Vergara, E., Meyer, M., & Goff, H. M. (1985) *Biochemistry 24*, 6561–6567.
Hammel, K. E., & Moen, M. A. (1991) *Enzyme Microb. Technol. 13*, 15–18.
Hammel, K. E., Kalyanaraman, B., & Kirk, T. K. (1986) *J. Biol. Chem. 261*, 16948–16952.
Hochmann, J., & Kellerhalls, H. P. (1980) *J. Magn. Reson. 38*, 23–29.
Inubushi, T., & Becker, E. D. (1983) *J. Magn. Reson. 51*, 128–133.
Kersten, P. J., Kalyanaraman, B., Hammel, K. E., Reinhammer, B., & Kirk, T. K. (1990) *Biochem. J. 268*, 475–480.
Kirk, T. K., & Farrell, R. L. (1987) *Annu. Rev. Microbiol. 41*, 465–505.
Kirk, T. K., Croan, S., Tien, M., Murtagh, K. E., & Farrell, R. L. (1985) *Enzyme Microb. Technol. 8*, 27–32.
La Mar, G. N. (1979) in *Biological Applications of Magnetic Resonance* (Shulman, R. G., Ed.) pp 305–343, Academic Press, New York.
La Mar, G. N., & de Ropp, J. S. (1979) *Biochem. Biophys. Res. Commun. 90*, 36–41.
La Mar, N., & Walker, F. A. (1979) in *The Porphyrins* (Dolphin, D., Ed.) Part IV-B, pp 61–157, Academic Press, New York.
La Mar, G. N., & de Ropp, J. S. (1982) *J. Am. Chem. Soc. 104*, 5203–5206.
Lukat, G. S., Rodgers, K. R., Jabro, M. N., & Goff, H. M. (1989) *Biochemistry 28*, 3338–3345.
Macura, S., Wüthrich, K., & Ernst, R. R. (1982) *J. Magn. Reson. 47*, 351–357.
Marion, D. & Wüthrich, K. (1983) *Biochem. Biophys. Res. Commun. 113*, 962–974.
Millis, C. D., Cai, D., Stankovich, M. T., & Tien, M. (1989) *Biochemistry 28*, 8484–8489.
Mincey, T., & Traylor, T. G. (1979) *J. Am. Chem. Soc. 101*, 765–766.
Morishima, I., Ogawa, S., Inubushi, T., Yonezawa, T., & Iizuka, T. (1977) *Biochemistry 16*, 5109–5115.
Neuhaus, D., & Williamson, M. (1989) *The Nuclear Overhauser Effect in Structural and Conformational Analysis*, VCH, New York.
Pease, E. A., Andrawis, A., & Tien, M. (1989) *J. Biol. Chem. 264*, 13531–13535.
Pribnow, D., Mayfield, M. B., Nipper, V. J., Brown, J. A., & Gold, M. H. (1989) *J. Biol. Chem. 264*, 5036–5040.
Poulos, T. L., & Kraut, J. (1980) *J. Biol. Chem. 255*, 8199–8205.
Quinn, R., Mercer-Smith, J., Burstyn, J., & Valentine, J. S. (1984) *J. Am. Chem. Soc. 106*, 4136–4144.
Ramaprasad, S., Jonhson, R. D., & La Mar, G. N. (1984) *J. Am. Chem. Soc. 106*, 3632–3635.
Satterlee, J. D. (1987) in *Metal Ions in Biological Systems* (Sigel, H., Ed.) Vol. 21, pp 121–185, Marcel Dekker, New York.
Satterlee, J. D., & Erman, J. E. (1991) *Biochemistry 30*, 4398–4405.
Satterlee, J. D., Erman, J. E., La Mar, G. N., Smith, K. M., & Langry, K. C. (1983) *Biochim. Biophys. Acta 743*, 246–255.
Satterlee, J. D., Erman, J. E., & de Ropp, J. S. (1987) *J. Biol. Chem. 262*, 11578–11583.
Satterlee, J. D., Erman, J. E., Mauro, J. M., & Kraut, J. (1990) *Biochemistry 29*, 8797–8806.
Satterlee, J. D., Russell, D. J., & Erman, J. E. (1991) *Biochemistry 30*, 9072–9077.
Shulman, G., Glarum, S. H., & Karplus, M. (1971) *J. Mol. Biol. 57*, 93–115.
Smulevich, G., Mauro, J. M., Fishel, L. F., English, A. M., Kraut, J., & Spiro, T. G. (1988) *Biochemistry 27*, 5477–5485.
Smulevich, G., Miller, M. A., Kraut, J., & Spiro, T. G. (1991) *Biochemistry 30*, 9546–9558.
Suslick, K. S., Fox, M. M., & Reinert, T. (1984) *J. Am. Chem. Soc. 106*, 4522–4525.
Takano, T. (1977) *J. Mol. Biol. 110*, 537–568.
Takio, K., Titani, K., Ericsson, L. H., & Yonetani, T. (1980) *Arch. Biochem. Biophys. 203*, 615–629.
Thanabal, V., de Ropp, J. S., & La Mar, G. N. (1986) *J. Am. Chem. Soc. 108*, 4244–4245.
Thanabal, V., de Ropp, J. S., & La Mar, G. N. (1987a) *J. Am. Chem. Soc. 109*, 265–272.
Thanabal, V., de Ropp, J. S., & La Mar, G. N. (1987b) *J. Am. Chem. Soc. 109*, 7516–7525.
Thanabal, V., de Ropp, J. S., & La Mar, G. N. (1988a) *J. Am. Chem. Soc. 110*, 3027–3035.
Thanabal, V., La Mar, G. N., & de Ropp, J. S. (1988b) *Biochemistry 27*, 5400–5407.
Tien, M. (1987) *CRC Crit. Rev. Microbiol. 15*, 141–168.
Tien, M., & Kirk, T. K. (1983) *Science 221*, 661–663.
Tien, M., & Tu, C.-P. D. (1987) *Nature 326*, 520–523.
Tien, M., & Myer, S. B. (1990) *Appl. Environ. Microbiol. 56*, 2540–2544.
Traylor, T. G., & Popovitiz-Biro, R. (1988) *J. Am. Chem. Soc. 110*, 239–243.
Traylor, T. G., White, D. K., Campbell, D. H., & Berzinis, A. P. (1981) *J. Am. Chem. Soc. 103*, 4932–4936.
Vold, R. L., Waugh, J. S., Klein, M. P., & Phelps, D. E. (1968) *J. Chem. Phys. 48*, 3831–3832.
Wariishi, H., Valli, K., & Gold, M. H. (1991) *Biochem. Biophys. Res. Commun. 176*, 269–275.
Yamamoto, Y., Osawa, A., Inoue, Y., Chujo, R., & Suzuki, T. (1989) *FEBS Lett. 247*, 263–267.
Yamamoto, Y., Nanai, N., Chujo, R., & Suzuki, T. (1990) *FEBS Lett. 264*, 113–116.
Yamamoto, Y., Chujo, R., & Suzuki, T. (1991) *Eur. J. Biochem. 198*, 285–291.
Yu, L. P., La Mar, G. N., & Rajanathnam, K. (1990) *J. Am. Chem. Soc. 112*, 9527–9534.

Registry No. MnP, 114995-15-2; LiP, 42613-30-9.